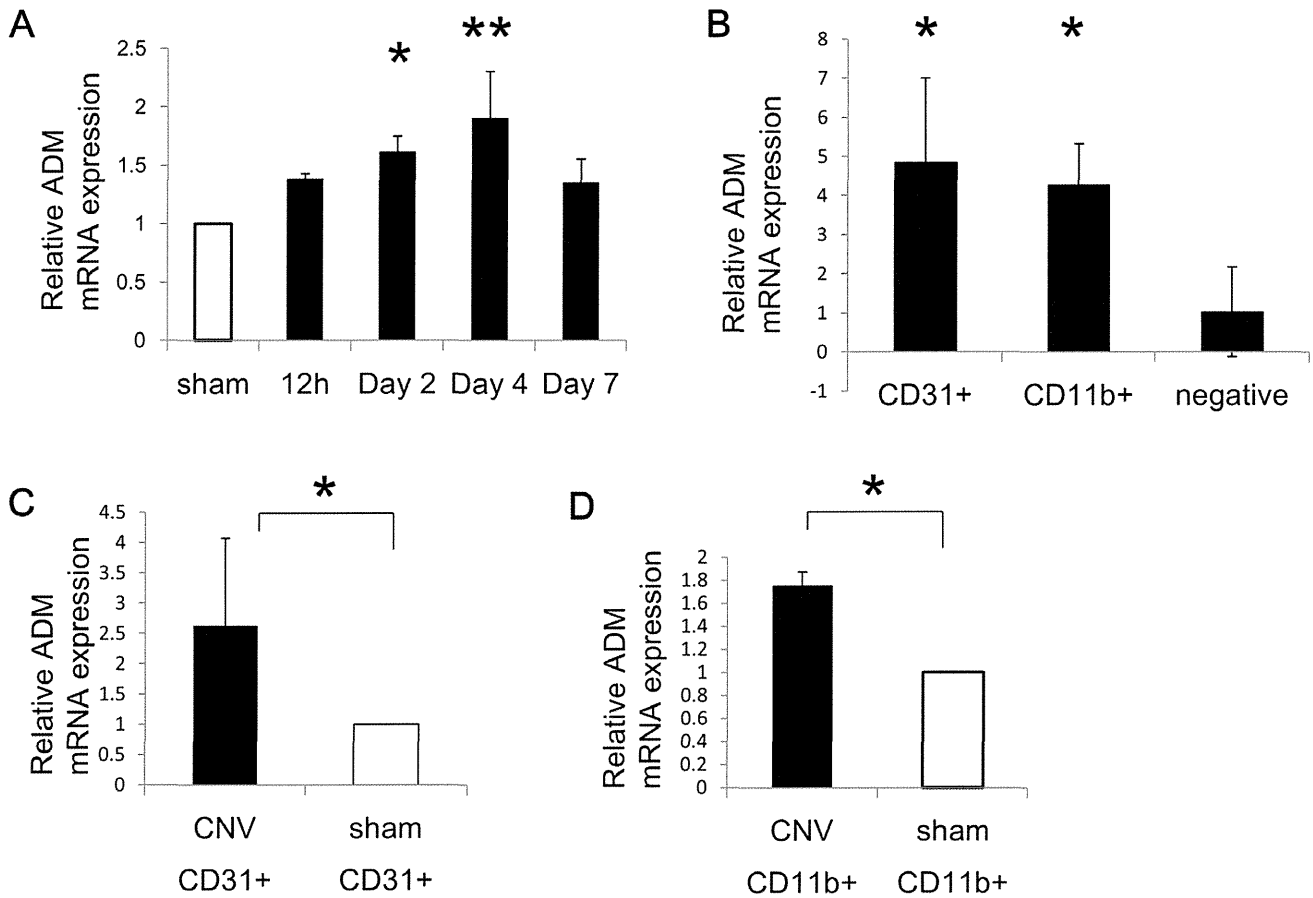

Figure 2. ADM expression after laser treatment. (A) Time course ADM mRNA expression by qRT–PCR analysis in the RPE/choroid complex after laser treatment. Results are shown as fold-increase in comparison with RPE/choroid complexes from sham-operated eyes. (B) qRT–PCR analysis of ADM mRNA expression in sorted CD31$^+$ cells (EC-enriched cell population), CD11b$^+$ cells (monocyte/macrophage lineage cells) and cells negative for either CD31 or CD11b (non-EC, non-monocyte/macrophage lineage fraction) 3 days after laser treatment ($n \geq 5$). (C) qRT–PCR analysis of ADM mRNA expression in sorted CD31$^+$ cells after laser treatment (CNV) compared to sham-treated eyes (sham). ($n \geq 5$, *$P<0.05$) (D) qRT–PCR analysis of ADM mRNA expression in sorted CD11b$^+$ cells after laser treatment compared to sham-treated eyes. ($n \geq 5$, *$P<0.05$).
doi:10.1371/journal.pone.0058096.g002

viously [18]. Image J for Windows (NIH, Bethesda, Maryland) analysis software was used to measure the area of CNV, with the operator blinded with respect to treatment groups.

Flow Cytometry (Analysis and Cell Sorting)

Procedures for cell preparation and staining were as previously reported [19]. Briefly, eyes from at least 5 mice which were laser coagulated or not were extracted and the RPE-choroid complex were gently scraped off the sclera. The RPE-complex was digested with collagenase (Wako, Osaka, Japan), and type II collagenase (Worthington Biochemical Corp., Lakewood, New Jersey) at 37°C. The digested tissue was passed through 40-μm filters to yield single cell suspensions. Cell surface antigen staining was performed as described previously [20]. Anti-CD45, -CD31, -CD11b (Pharmingen, BD Biosciences) mAbs were used for immunofluorescence staining. The stained cells were analyzed and sorted using a FACSAria flow cytometer (BD) with FlowJo (TreeStar) software. Dead cells were excluded from the analyses using the 2D profile of forward versus side scatter.

Quantitative Reverse-transcription Real-time PCR (qRT-PCR)

For RNA extraction, we used at least 5 mice in each group for sorted cells as indicated above. For analysis of ADM mRNA expression in RPE/choroid complexes, we used 2 mice per day. RNA was extracted from cells using an RNeasy Mini Kit (Qiagen), and cDNA was generated using reverse transcriptase from the ExScript RT reagent Kit (Perfect Real Time) (Takara). Real-time PCR was performed using a Stratagene Mx3000P (Stratagene, La Jolla, CA). Polymerase chain reaction (PCR) was performed on cDNA using specific primers following; mouse CRLR, 5′-ACC TGC ACA CAC TCA TCG TG-3′ and 5′-TGA TCC AGC AAT TGT CGT TG-3′; mouse RAMP2, 5′-CTG AGG ACA GCC TTG TGT CA-3′ and 5′-AAG TCC AGT TGC ACC AGT CC-3′; mouse RAMP3, 5′-AAG GTG GCT GTC TGG AAG TG-3′ and 5′-TGA TGT TGG TCT CCA TCT CG′; mouse ADM, 5′- GAC TCG CTG ATG AGA CGA CA-3′ and 5′- GAA CCC TGG TTC ATG CTC TG′; mouse GAPDH, 5′-TGG CAA AGT GGA GAT TGT TGC C-3′ and 5′- AAG ATG GTG ATG GGC TTC CCG-3′; human ADM, 5′- ATG AAG GGT GCC TCT CGA A-3′ and 5′- CCC TGG AAG TTG TTC ATG C-3′; human GAPDH, 5′- GAA GGT GAA GGT CGG AGT C-3′ and 5′- GAA GAT GGT GAT GGG ATT TC-3′.

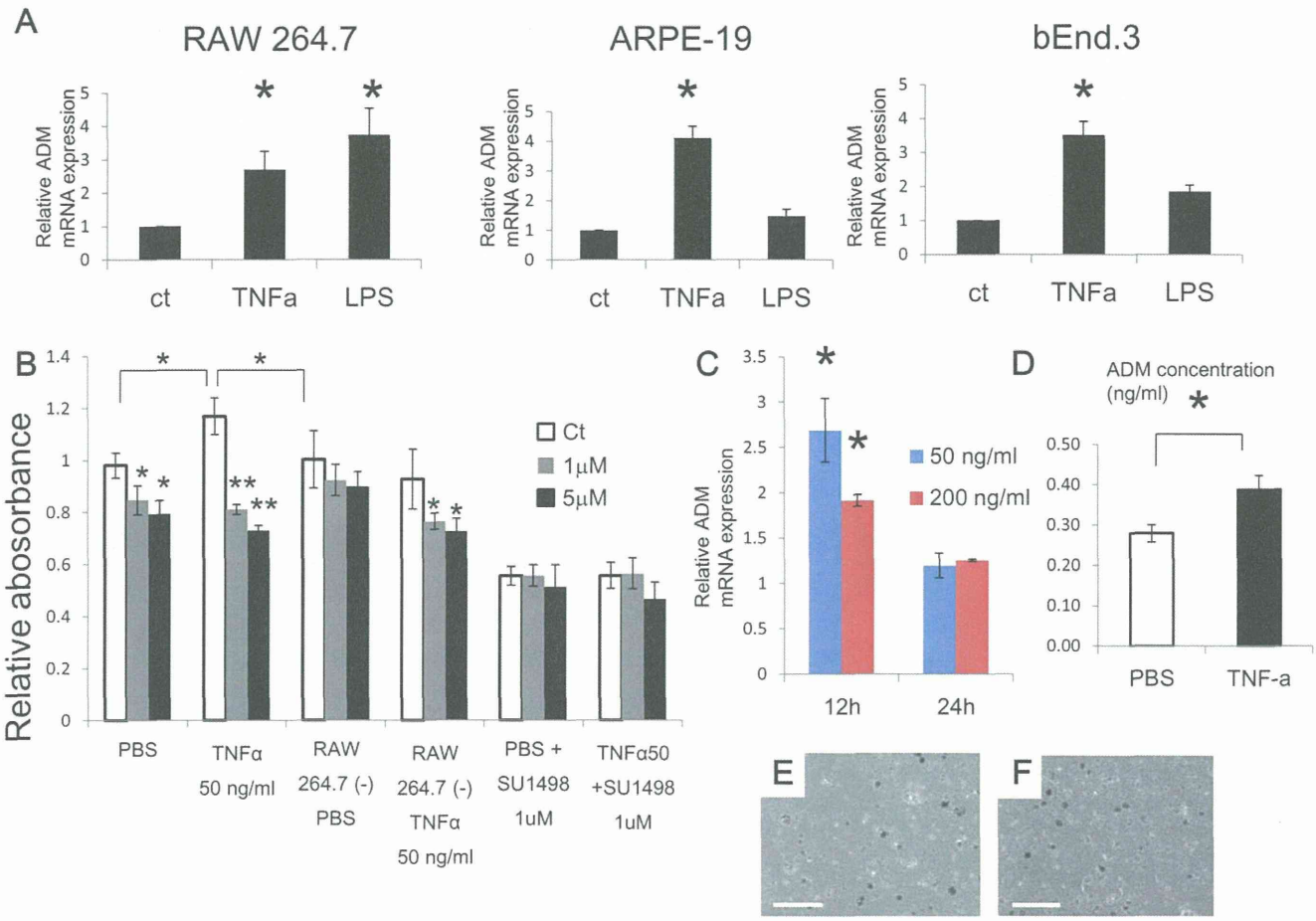

Figure 3. In vitro effect of an ADM antagonist. (A) qRT–PCR analysis of ADM mRNA expression after 12 h**r** TNF-α or LPS stimulation of cells, as indicated (n = 3, *P<0.01). (B) EC proliferation assay using bEND.3 which was incubated with or without supernatant from TNF-α-stimulated RAW 264.7 in the presence or absence of the ADM antagonist ADM (22–52). The white bar indicates the PBS group, gray indicates the 1 μM ADM (22–52) group and black the 5 μM ADM (22–52) group. ECs in all groups were incubated with supernatant from RAW 264.7 cells except for RAW 264.7 (-) groups (culture medium without supernatant of RAW 264.7 cells). 1 μM SU1498 was added to indicated groups (n = 3, **P<0.01, *P<0.05). (C) qRT–PCR analysis of ADM mRNA expression after 12 and 24 hr TNF-α stimulation of primary RPE/choroid cultures (n = 3, *P<0.05). (D) ELISA of secreted ADM from primary RPE/choroid cultures after stimulation with 50 ng/ml TNF-α or culture with PBS alone (*P<0.05) (E, F) Appearance of primary RPE/choroid cultures after stimulation with PBS (E) or 50 ng/ml TNF-α(F). Scale bar: 100 μm.
doi:10.1371/journal.pone.0058096.g003

Expression level of the target gene was normalized to the GAPDH level in each sample.

In vitro Assays

We examined the in vitro effect of ADM on inflammatory responses of 3 major cell types associated with CNV formation, i.e., microvascular ECs, macrophages, and RPE cells, using the murine cell lines bEnd3, RAW264.7, and the human cell line ARPE-19, respectively. ARPE19 cells were purchased from the American Type Culture Collection (ATCC, Manassas, VA). Cells were cultured in six-well plates for 12 hours in DMEM (Sigma, ATCC and Nikken, respectively). After 4 hours serum starvation using 0.5% fetal bovine serum (FBS), cells were stimulated with tumor necrosis factor (TNF)-α (PeproTech, 50 ng/mL) or lipopolysaccharide (LPS; Wako, 10 μg/mL). After a 12 hour incubation, cell lysate from each line, and the supernatants from cultures of RAW264.7 cells, were processed for real-time RT PCR and EC proliferation assays, respectively. ECs (bEnd3) which were incubated for an additional 4 hours with supernatant plus 1 μM or 5 μM ADM (22–52), or PBS, were quantified using Cell-counting kit-8 (DOJINDO) according to the supplier's protocol. 1 μM SU1498 was added to the supernatant in some experiments. Dose-response model assessing the toxicity of ADM (22–52) was also performed using same kit after 24 hour incubation of ADM inhibitor at indicated concentration. Absorbance was then measured at 490 nm, and at 630 nm as reference, with a Microplate Reader 550 (Bio-Rad Laboratories). Primary culture of RPE/choroid complexes was performed using cells dissected from 8-week-old wild-type C57BL/6 mice. Tissues were dissociated with trypsin, resuspended in DMEM containing 20% FBS and then plated on laminin-coated 24-well plates at a density of a tissue from1 mouse/well and incubated at 37°C, 5% CO_2 for 24 h before 4 hours serum starvation with 0.5% FBS. After 12 hours TNF-α treatment, tissues were collected and immediately washed with PBS before RNA extraction. For ELISA, after seeding the primary culture, we cultured for 24 hours as indicated above, then serum-starved for 4 hours in DMEM without FBS before TNF-α stimulation. We stimulated cells with 50 ng/ml TNF-α for 24 hours without FBS. We used an ADM detection kit (Phoenix Pharmaceuticals) according to the supplier's protocol.

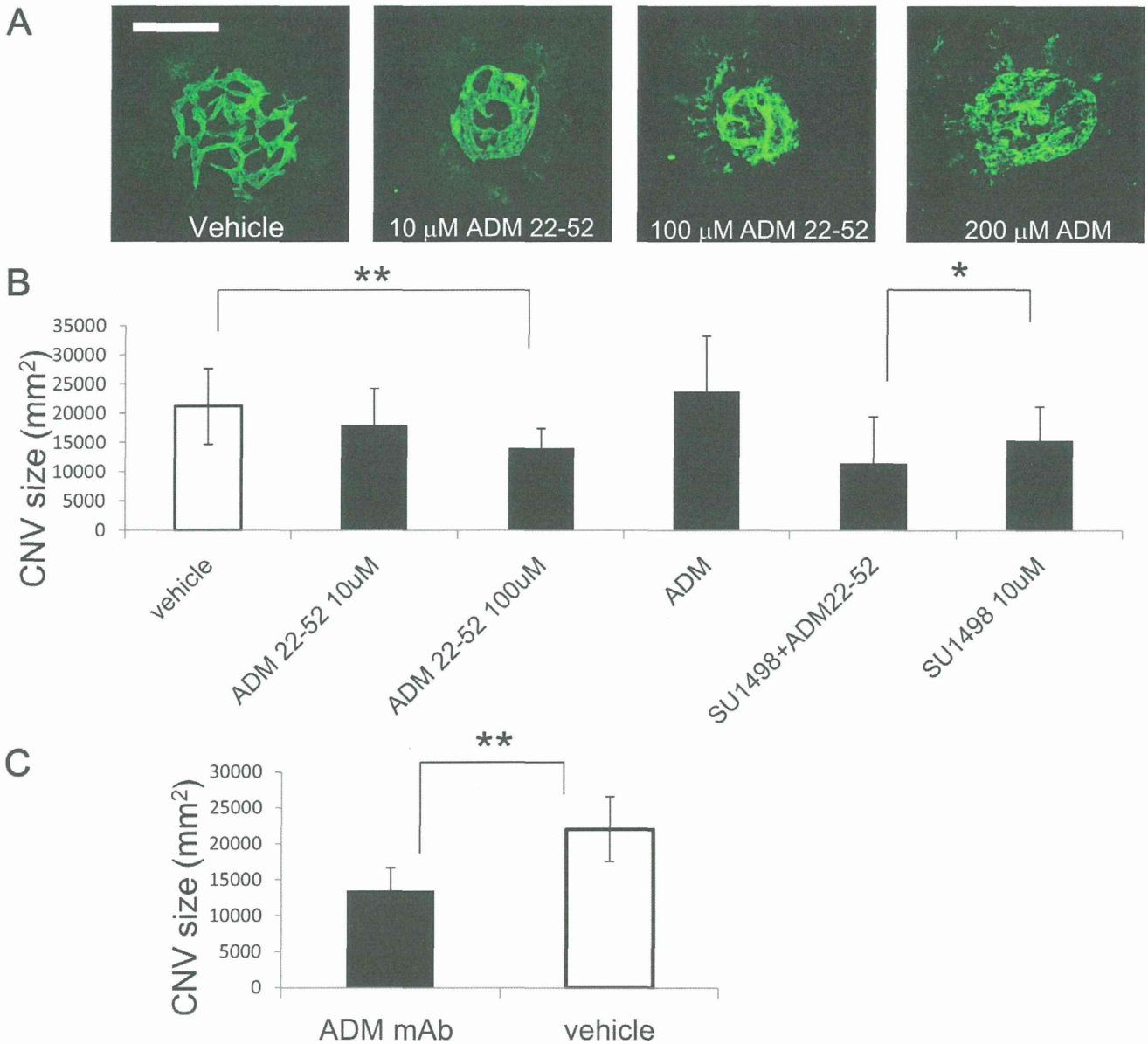

Figure 4. Suppression of CNV in mice by blocking ADM. (A) Flat-mount immunofluorescence staining with anti-PECAM-1/CD31 antibody in the choroid after vehicle, ADM (22–52) or recombinant ADM treatment. Scale bar: 100 μm. (B) Quantitative analysis of CNV size as revealed in (A). (n = 16, **P<0.01) and quantitative analysis of CNV size after treatment with 10 μM SU1498 with or without 100 μM ADM (22–52) (n = 8, *P<0.05). (C) Quantitative analysis of CNV size treated with ADM mAb compared to vehicle. (n = 10, **P<0.01). Error bars indicate mean ± s.d.
doi:10.1371/journal.pone.0058096.g004

Immunohistochemistry

The procedure for tissue preparation and staining was as previously reported [21]. For immunohistochemistry, biotin-conjugated anti-CD31 antibody (BD Biosciences, 1:200) was used for staining and anti-rat IgG Alexa Fluor 488 (Invitrogen, 1:300) as the secondary antibody. Samples were visualized using DM5500B (Leica) and confocal microscopy (TCS/SP5, Leica). Images were acquired with a DFC 500 digital camera (Leica) and processed with the Leica application suite (Leica) and Adobe Photoshop CS3 software (Adobe systems). All images shown are representative of more than 6 independent experiments.

Statistical Analysis

All data are presented as mean ± standard error of the mean (SEM). For statistical analysis, the statcel 2 software package (OMS) was used. In experiments involving qRT-PCR and CNV suppression with ADM mAb, we used two-sided Student's t-test to compare two groups (except for expression of ADM mRNA after CNV induction).We used analysis of variance performed on all data followed by Tukey–Kramer multiple comparison testing in qRT-PCR experiments for expression of ADM mRNA after CNV induction, EC proliferation assays using bEND.3 and for experiments on CNV suppression with ADM and VEGF antagonists. A probability value of less than 0.05 was considered statistically significant.

Results

To elucidate the involvement of ADM signaling in CNV, we first investigated the expression of the ADM receptor in choroidal vascular ECs in the CNV model. After we confirmed that CNV did not invade retinal tissue (Fig. 1A–D), $CD31^+CD45^-$ ECs in the RPE-choroid complex were analyzed by flow cytometry (Fig. 1E) and their number was calculated as a percentage of a total of 5×10^4 choroid/RPE complex cells 7 days after laser induction. We confirmed that the number of ECs increases after induction of CNV in laser-treated eyes (6.96% of total cells) compared to control eyes (4.57% of total cells) (Fig. 1F). There was no change in the number of $CD31^+$ $CD45^+$ or $CD31^-CD45^+$ cells; however, CD11b cells increased after laser-induction of CNV (6.32% vs 1.8%) (data not shown). Because ADM signaling is known to be mediated through CRLR/RAMP2 and CRLR/RAMP3 receptors, we analyzed the expression of CRLR, RAMP2 and RAMP3 mRNA in choroid/RPE complexes after induction of CNV. CRLR, RAMP2 and RAMP3 were highly expressed in the $CD31^+CD45^-$ ECs compared to $CD31^-CD45^-$ non-ECs. However, the level of expression of these ADM receptor components in ECs was not altered after CNV induction compared to sham-operated control groups (Fig. 1G). Moreover, we **c**onfirmed the expression of CRLR in the ECs of CNV by immunostaining (Fig. 1H).

Next, we assessed the expression of ADM during CNV formation. In the laser-induced CNV model, the presence of different angiogenic factors in RPE-Choroid complexes has already been reported [22]. We analyzed the expression of ADM mRNA and found that it increased in a time-dependent fashion and peaked 4 days after laser treatment (Fig. 2A). Because it is reported that ADM promotes angiogenesis in both an autocrine and a paracrine manner [8,23], we focused on two cell populations which could be isolated by flow cytometry: $CD31^+$ ECs and $CD11b^+$ monocytes/macrophages. We confirmed that both ECs and macrophages express more ADM mRNA compared to $CD31^-CD11b^-$ cells (Fig. 2B). Furthermore, after CNV induction, ADM expression was significantly upregulated in both ECs and macrophages compared to the same cells in sham-operated mice (Fig. 2C, D). Therefore, these data suggest that ADM is involved in this laser-induced CNV model.

It is well known that inflammatory cytokines upregulate ADM expression in various cells [24,25,26]. We confirmed this by using macrophage (RAW264.7), EC (bEnd.3), and retinal pigment epithelial (ARPE-19) cell lines stimulated with TNF-α and LPS (Fig. 3A). It has been reported that ADM induces EC proliferation, migration and tube formation through phosphatidylinositol 3′ kinase (PI 3′ -kinase)/Akt, extracellular signal-regulated kinase (ERK), and tyrosine phosphorylation of focal adhesion kinase (p125 FAK) [14]. Thus, we tested whether culture supernatant from RAW264.7 cells after TNF-α stimulation promotes EC proliferation and whether this can be inhibited by a widely-accepted ADM antagonist, ADM (22–52) [27]. Although the inhibitory effect was weak compared to a potent VEGF-A signaling inhibitor, SU1498 [28], ADM (22–52) did significantly suppress proliferation of EC cultured not only in supernatant from TNF-α-stimulated macrophages but also to some extent in medium containing TNF-α without macrophages (Fig. 3B). Additionally, we confirmed the absence of the potential toxicity of ADM (22–52) using an in vitro dose-response model (Fig. S1). These data suggest that ADM signaling affects EC proliferation in an autocrine and a paracrine manner. Moreover, we evaluated the expression of ADM in 24 hour-cultured primary RPE/choroid complexes obtained from wild-type mice. TNF-α stimulation of cultured primary RPE/choroid complexes significantly upregulated ADM mRNA and protein levels at the 12 hour time point (Fig. 3C and 3D); however, expression of ADM mRNA after 24 hours was downregulated relative to the 12 hour time point (Fig. 3C). The morphology of the cells did not change(Fig. 3E and 3F).

To clarify the role of ADM in this CNV model, we inhibit ADM signaling using intraocular injections of ADM antagonist, ADM (22–52). Quantification of CNV size judged by immunohistochemical analysis with anti-PECAM-1 Ab 7 days after laser treatment revealed that intraocular injection of ADM (22–52) significantly inhibited the formation of CNV to approximately 60% of controls. In contrast, injection of recombinant ADM did not affect the size of CNV compared to controls, contrary to our expectations (Fig. 4A and B). This suggests that an excessive amount of ADM is produced in the choroid/RPE in this CNV model. Next, we assessed whether the ADM antagonist had any synergistic effect with SU1498 on CNV. Treatment with ADM antagonist and SU1498 together suppressed CNV formation more than SU1498 alone (Fig. 4C). Furthermore, we confirmed the effect of anti-ADM monoclonal antibody; intraocular injection of ADM mAb resulted in significant suppression of CNV formation (Fig. 4D).

Discussion

In the current study, we have explored the possibility that ADM exerts angiogenic effects in a laser-induced CNV model. The ADM receptor was expressed in choroidal endothelial cells and ADM was upregulated in the choroid/RPE complex during CNV formation. Moreover, an ADM pharmaceutical antagonist and a mAb to ADM efficiently suppressed CNV formation and mediated synergistic effects together with a potent VEGF-A inhibitor. These findings suggest that ADM could represent a therapeutic target and be an attractive option for the treatment of CNV in AMD.

The biological functions of ADM are well- recognized to be dilatation of resistance vessels [29,30], increases of cardiac output [31], regulation of vascular permeability [32] and contribution to mobilization, adhesion and differentiation into endothelial progenitor cells of bone marrow-derived cells [33,34,35]. Additionally, several lines of evidence have suggested that inhibiting the ADM pathway with antibodies or antagonists directed against ADM or ADM receptors can reduce angiogenesis and tumor cell proliferation in mouse cancer models [8]. Although ADM is reported to affect not only angiogenesis but also tumor cell proliferation via its autocrine and paracrine mechanisms in cancer, there is little data showing the involvement of ADM in a disease model whose central pathogenesis depends on sprouting angiogenesis [11,12,13,16,23].

ADM immunoreactivity was reported in cardiac myocytes, vascular smooth muscle cells, ECs, renal distal and collecting tubules, mucosal and glandular epithelia of the digestive, respiratory and reproductive system, the endocrine and neuroendocrine system, as well as in the central nervous system [29]. In the current model, upregulation of ADM was not detected in the retina after laser treatment (data not shown), although Blom et al. reported the expression of ADM in neural retina. However, we saw ADM in the RPE/choroid. Secreted inflammatory cytokines after laser burn might be enhancing ADM expression and further accumulation of inflammatory cells.

This was confirmed using a primary RPE/choroid culture model in the present study. However, ADM expression 24 hr after TNF-α stimulation was lower than at 12 hr, in contrast to findings

with different cell lines such as RAW 264.7, RPE-19 and bEnd.3. We hypothesize that this difference can be attributed to the use of transformed cell lines which could display different expression patterns compared to that of primary cultures. Local upregulation of ADM at each photocoagulated site could induce direct ADM effects, i.e. EC proliferation, migration and tube formation. Currently, anti-VEGF therapy has become the major treatment modality for neovascular AMD. However, numerous injections of the anti-VEGF drug may be required to maintain clinical benefit. Moreover, after treatment with anti-VEGF drugs, it can be hypothesized that a hypoxic response could occur and subsequently upregulate ADM, because this has been observed in ECs [25] [36]. Chen et al. reported reciprocal regulation of ADM and HIF-1α expression exerted synergistic effects on proliferation of ECs in vitro [36]. Induction and nuclear translocation of HIF-1 α controls the expression of several angiogenic factors [37]. Therefore, the requirement for additional drugs together with anti-VEGF therapy is rational even if anti-ADM treatment partially suppresses CNV formation.

Although we expected that ADM injection would enhance the angiogenic response, exogenous ADM did not alter the size of CNV. We hypothesize that ADM was already saturated in the lesion and therefore additional factor would not be able to further activate the ADM receptor and exert any greater effects.

Chen et al. reported that tumor-associated macrophages (TAM) express both ADM and ADM receptor components. They also reported that ADM from TAM stimulated ECs and furthered angiogenesis via a paracrine pathway; moreover, it also potentiated the differentiation of TAM from the M1 to M2 state in an autocrine manner [23]. In the current study, infiltrating macrophages in CNV eyes expressed more ADM; therefore we cannot completely exclude the possibility that upregulation of ADM in macrophages could cause them to change their characteristics and to secrete other angiogenic factors such as VEGF. However, the finding of an inhibitory effect on EC proliferation of ADM antagonists in supernatant from macrophage cultures implies that ADM originating from macrophages must be at least partly responsible for CNV formation.

Udono et al. reported that hypoxia and inflammatory cytokines induced the expression of ADM in human RPE cells and that ADM could enhance RPE proliferation [26,38]. Therefore, in this CNV model, it is also possible that ADM expression in RPE was upregulated and that ADM secreted by RPE could promote angiogenesis. However, Huang et al. reported that ADM inhibited the migration of RPE cells in association with reductions in $[Ca^{2+}]$ [39]. Although there is some controversy about the function of ADM in RPE cells, we could demonstrate that inflammatory stimulation up-regulated the expression of ADM in RPE in vitro. Indeed, it is technically difficult to sort the RPE cells by flow cytometry using specific surface markers and we were unable to determine their ADM expression level. Although we have to carefully evaluate the major source of ADM in the CNV model, the observed paracrine and autocrine effects of ADM could induce CNV.

Supporting Information

Figure S1 Toxicity experiment of ADM (22–52) using bEnd.3. proliferation assay. ADM (22–52) could inhibit the proliferation of EC at 10 nM but there was no clear toxicity even at concentration of 100 μM. (*P<0.05).
(TIF)

Acknowledgments

We thank Keisho Fukuhara and Noriko Fujimoto for general assistance.

Author Contributions

Conceived and designed the experiments: SS MK KN NT. Performed the experiments: SS HK HN TW HS. Analyzed the data: SS HK NT DY. Contributed reagents/materials/analysis tools: SS MK KN NT. Wrote the paper: SS NT.

References

1. Dewan A, Liu M, Hartman S, Zhang SS, Liu DT, et al. (2006) HTRA1 promoter polymorphism in wet age-related macular degeneration. Science 314: 989–992.
2. Sakurai E, Anand A, Ambati BK, van Rooijen N, Ambati J (2003) Macrophage depletion inhibits experimental choroidal neovascularization. Invest Ophthalmol Vis Sci 44: 3578–3585.
3. Tsutsumi-Miyahara C, Sonoda KH, Egashira K, Ishibashi M, Qiao H, et al. (2004) The relative contributions of each subset of ocular infiltrated cells in experimental choroidal neovascularisation. Br J Ophthalmol 88: 1217–1222.
4. Xie P, Kamei M, Suzuki M, Matsumura N, Nishida K, et al. (2011) Suppression and regression of choroidal neovascularization in mice by a novel CCR2 antagonist, INCB3344. PLoS One 6: e28933.
5. Xiong M, Elson G, Legarda D, Leibovich SJ (1998) Production of vascular endothelial growth factor by murine macrophages: regulation by hypoxia, lactate, and the inducible nitric oxide synthase pathway. Am J Pathol 153: 587–598.
6. Poyner DR, Sexton PM, Marshall I, Smith DM, Quirion R, et al. (2002) International Union of Pharmacology. XXXII. The mammalian calcitonin gene-related peptides, adrenomedullin, amylin, and calcitonin receptors. Pharmacol Rev 54: 233–246.
7. McLatchie LM, Fraser NJ, Main MJ, Wise A, Brown J, et al. (1998) RAMPs regulate the transport and ligand specificity of the calcitonin-receptor-like receptor. Nature 393: 333–339.
8. Nikitenko LL, Fox SB, Kehoe S, Rees MC, Bicknell R (2006) Adrenomedullin and tumour angiogenesis. Br J Cancer 94: 1–7.
9. Iimuro S, Shindo T, Moriyama N, Amaki T, Niu P, et al. (2004) Angiogenic effects of adrenomedullin in ischemia and tumor growth. Circ Res 95: 415–423.
10. Shindo T, Kurihara Y, Nishimatsu H, Moriyama N, Kakoki M, et al. (2001) Vascular abnormalities and elevated blood pressure in mice lacking adrenomedullin gene. Circulation 104: 1964–1971.
11. Ishikawa T, Chen J, Wang J, Okada F, Sugiyama T, et al. (2003) Adrenomedullin antagonist suppresses in vivo growth of human pancreatic cancer cells in SCID mice by suppressing angiogenesis. Oncogene 22: 1238–1242.
12. Kaafarani I, Fernandez-Sauze S, Berenguer C, Chinot O, Delfino C, et al. (2009) Targeting adrenomedullin receptors with systemic delivery of neutralizing antibodies inhibits tumor angiogenesis and suppresses growth of human tumor xenografts in mice. FASEB J 23: 3424–3435.
13. Ouafik L, Sauze S, Boudouresque F, Chinot O, Delfino C, et al. (2002) Neutralization of adrenomedullin inhibits the growth of human glioblastoma cell lines in vitro and suppresses tumor xenograft growth in vivo. Am J Pathol 160: 1279–1292.
14. Kim W, Moon SO, Sung MJ, Kim SH, Lee S, et al. (2003) Angiogenic role of adrenomedullin through activation of Akt, mitogen-activated protein kinase, and focal adhesion kinase in endothelial cells. FASEB J 17: 1937–1939.
15. Ribatti D, Nico B, Spinazzi R, Vacca A, Nussdorfer GG (2005) The role of adrenomedullin in angiogenesis. Peptides 26: 1670–1675.
16. Hague S, Zhang L, Oehler MK, Manek S, MacKenzie IZ, et al. (2000) Expression of the hypoxically regulated angiogenic factor adrenomedullin correlates with uterine leiomyoma vascular density. Clin Cancer Res 6: 2808–2814.
17. Gavard J, Hou X, Qu Y, Masedunskas A, Martin D, et al. (2009) A role for a CXCR2/phosphatidylinositol 3-kinase gamma signaling axis in acute and chronic vascular permeability. Mol Cell Biol 29: 2469–2480.
18. Campa C, Kasman I, Ye W, Lee WP, Fuh G, et al. (2008) Effects of an anti-VEGF-A monoclonal antibody on laser-induced choroidal neovascularization in mice: optimizing methods to quantify vascular changes. Invest Ophthalmol Vis Sci 49: 1178–1183.
19. Naito H, Kidoya H, Sakimoto S, Wakabayashi T, Takakura N (2011) Identification and characterization of a resident vascular stem/progenitor cell population in preexisting blood vessels. EMBO J 31: 842–855.
20. Takakura N, Watanabe T, Suenobu S, Yamada Y, Noda T, et al. (2000) A role for hematopoietic stem cells in promoting angiogenesis. Cell 102: 199–209.

21. Sakimoto S, Kidoya H, Naito H, Kamei M, Sakaguchi H, et al. (2012) A role for endothelial cells in promoting the maturation of astrocytes through the apelin/APJ system in mice. Development 139: 1327–1335.
22. Grossniklaus HE, Kang SJ, Berglin L (2010) Animal models of choroidal and retinal neovascularization. Prog Retin Eye Res 29: 500–519.
23. Chen P, Huang Y, Bong R, Ding Y, Song N, et al. (2011) Tumor-associated macrophages promote angiogenesis and melanoma growth via adrenomedullin in a paracrine and autocrine manner. Clin Cancer Res 17: 7230–7239.
24. Kubo A, Minamino N, Isumi Y, Katafuchi T, Kangawa K, et al. (1998) Production of adrenomedullin in macrophage cell line and peritoneal macrophage. J Biol Chem 273: 16730–16738.
25. Ogita T, Hashimoto E, Yamasaki M, Nakaoka T, Matsuoka R, et al. (2001) Hypoxic induction of adrenomedullin in cultured human umbilical vein endothelial cells. J Hypertens 19: 603–608.
26. Udono T, Takahashi K, Nakayama M, Murakami O, Durlu YK, et al. (2000) Adrenomedullin in cultured human retinal pigment epithelial cells. Invest Ophthalmol Vis Sci 41: 1962–1970.
27. Saita M, Shimokawa A, Kunitake T, Kato K, Hanamori T, et al. (1998) Central actions of adrenomedullin on cardiovascular parameters and sympathetic outflow in conscious rats. Am J Physiol 274: R979–984.
28. Boguslawski G, McGlynn PW, Harvey KA, Kovala AT (2004) SU1498, an inhibitor of vascular endothelial growth factor receptor 2, causes accumulation of phosphorylated ERK kinases and inhibits their activity in vivo and in vitro. J Biol Chem 279: 5716–5724.
29. Eto T (2001) A review of the biological properties and clinical implications of adrenomedullin and proadrenomedullin N-terminal 20 peptide (PAMP), hypotensive and vasodilating peptides. Peptides 22: 1693–1711.
30. Ishiyama Y, Kitamura K, Ichiki Y, Nakamura S, Kida O, et al. (1993) Hemodynamic effects of a novel hypotensive peptide, human adrenomedullin, in rats. Eur J Pharmacol 241: 271–273.
31. Rademaker MT, Charles CJ, Lewis LK, Yandle TG, Cooper GJ, et al. (1997) Beneficial hemodynamic and renal effects of adrenomedullin in an ovine model of heart failure. Circulation 96: 1983–1990.
32. Hippenstiel S, Witzenrath M, Schmeck B, Hocke A, Krisp M, et al. (2002) Adrenomedullin reduces endothelial hyperpermeability. Circ Res 91: 618–625.
33. Abe M, Sata M, Suzuki E, Takeda R, Takahashi M, et al. (2006) Effects of adrenomedullin on acute ischaemia-induced collateral development and mobilization of bone-marrow-derived cells. Clin Sci (Lond) 111: 381–387.
34. Iwase T, Nagaya N, Fujii T, Itoh T, Ishibashi-Ueda H, et al. (2005) Adrenomedullin enhances angiogenic potency of bone marrow transplantation in a rat model of hindlimb ischemia. Circulation 111: 356–362.
35. Kong XQ, Wang LX, Yang CS, Chen SF, Xue YZ, et al. (2008) Effects of adrenomedullin on the cell numbers and apoptosis of endothelial progenitor cells. Clin Invest Med 31: E117–122.
36. Chen L, Qiu JH, Zhang LL, Luo XD (2012) Adrenomedullin promotes human endothelial cell proliferation via HIF-1alpha. Mol Cell Biochem 365: 263–273.
37. Pugh CW, Ratcliffe PJ (2003) Regulation of angiogenesis by hypoxia: role of the HIF system. Nat Med 9: 677–684.
38. Udono T, Takahashi K, Nakayama M, Yoshinoya A, Totsune K, et al. (2001) Induction of adrenomedullin by hypoxia in cultured retinal pigment epithelial cells. Invest Ophthalmol Vis Sci 42: 1080–1086.
39. Huang W, Wang L, Yuan M, Ma J, Hui Y (2004) Adrenomedullin affects two signal transduction pathways and the migration in retinal pigment epithelial cells. Invest Ophthalmol Vis Sci 45: 1507–1513.

Graefes Arch Clin Exp Ophthalmol
DOI 10.1007/s00417-013-2505-2

RETINAL DISORDERS

Aqueous vascular endothelial growth factor and ranibizumab concentrations after monthly and bimonthly intravitreal injections of ranibizumab for age-related macular degeneration

Xiying Wang · Tomoko Sawada · Masashi Kakinoki · Taichiro Miyake Hajime Kawamura · Yoshitsugu Saishin · Ping Liu · Masahito Ohji

Received: 29 July 2013 / Revised: 7 October 2013 / Accepted: 16 October 2013

Abstract
Purpose To evaluate vascular endothelial growth factor (VEGF) and ranibizumab concentrations in eyes with age-related macular degeneration (AMD) after monthly and bimonthly intravitreal ranibizumab (IVR) injections.
Methods Aqueous humor samples were obtained from 26 eyes with AMD before and after IVR injections. Nine eyes received three monthly injections and 17 eyes received two bimonthly injections. The VEGF and ranibizumab concentrations were measured by enzyme-linked immunosorbent assay.
Results The aqueous VEGF concentrations in the monthly injection group decreased below the lowest detectable limit in eight of nine eyes 1 month after the first injection and seven of nine eyes 1 month after the second injection ($P<0.001$, mean baseline value, 94.7 pg/ml); the aqueous VEGF concentrations in the bimonthly injection group decreased below the lowest detectable limit in two of 17 eyes 2 months after the first injection ($P<0.001$, mean baseline value, 152.4 pg/ml). The mean aqueous ranibizumab concentrations with monthly injections were 71.2 ng/ml 1 month after the first injection, and 96.3 ng/ml 1 month after the second injection. The mean aqueous ranibizumab concentrations in the bimonthly injection group were 2.5 ng/ml in 15 of 17 eyes, and below the lowest detectable limit in two of 17 eyes 2 months after the first injection.
Conclusions In this pilot study with limited follow-up, intravitreal injection of ranibizumab can suppress aqueous VEGF completely for 1 month in most cases. Its effect does not last for 2 months enough to suppress VEGF completely in most cases, although aqueous VEGF at 2 months after intravitreal injection of ranibizumab is less than that before injection in most cases.

Keywords Age-related macular degeneration · Aqueous humor · Ranibizumab · Bimonthly intravitreal injection · Vascular endothelial growth factor

Introduction

Vascular endothelial growth factor (VEGF) plays a key role in the development of neovascularization in exudative age-related macular degeneration (AMD) [1–7], the leading cause of irreversible blindness among aging populations in developed countries [8–11]. The aqueous VEGF concentration in eyes with AMD and polypoidal choroidal vasculopathy (PCV) increases compared with normal eyes [12–16].

Ranibizumab (Lucentis, Genentech Inc., South San Francisco, CA, USA) is a recombinant, humanized monoclonal antibody Fab fragment that neutralizes all biologically active forms of VEGF-A. Anti-VEGF therapy with ranibizumab significantly decreased the VEGF concentrations in the aqueous humor of eyes with AMD [14–16]. Monthly injections of 0.5 mg of ranibizumab prevent visual loss, and the mean visual acuity (VA) increased after 2 years in patients with all types of

The Institutional Review Board of Shiga University of Medical Science Hospital approved this study, which is registered at http://www.umin.ac.jp (No. UMIN000005691). All patients provided informed written consent before participation.

X. Wang · T. Sawada (✉) · M. Kakinoki · T. Miyake · H. Kawamura · Y. Saishin · M. Ohji
Department of Ophthalmology, Shiga University of Medical Science, Seta Tukinowacho, Otsu, Shiga 520-2192, Japan
e-mail: tsawada@belle.shiga-med.ac.jp

X. Wang · P. Liu
Key Laboratory of Harbin Medical University Eye Center, Eye Hospital, First Affiliated Hospital, Harbin Medical University, Harbin, People's Republic of China

Published online: 07 November 2013

choroidal neovascularization (CNV) secondary to AMD [17–19]. It is unclear if monthly intravitreal ranibizumab (IVR) injections are needed. Monthly injections may increase the risk of intraocular infection and impose a heavy economic burden on patients. Some investigators administered quarterly IVR injections after three monthly loading doses to treat AMD, but this regimen did not achieve noninferiority to monthly injections, which means that a regimen with more frequent drug administration is needed [20–22].

Increasing interest also has focused on aflibercept (VEGF Trap-Eye, Regeneron Pharmaceuticals, Tarrytown, NY, USA). Unlike ranibizumab and bevacizumab (Avastin, Genentech Inc.), aflibercept is a recombinant fusion protein comprised of portions of human VEGFR1 and VEGFR2 extracellular domains fused to the Fc portion of human immunoglobulin G1 [23, 24]. With an extraordinarily high VEGF binding affinity, aflibercept binds all VEGF-A, VEGF-B, and placental growth factor. The VIEW I and VIEW 2 studies, two parallel, phase III, double-masked, randomized, multicenter trials, evaluated the efficacy and safety of bimonthly injections of aflibercept after three monthly injections of the drug, compared with monthly injections of ranibizumab. The results indicated that bimonthly injections of aflibercept were not inferior to monthly injections of ranibizumab over a 1-year period [25]. However, little data are available on bimonthly injections of ranibizumab. The current study investigated the aqueous VEGF and ranibizumab concentrations in patients with AMD after monthly and bimonthly IVR injections.

Material and methods

Patients

Twenty-six eyes of 26 patients were enrolled between August 2009 and August 2012. The monthly injection group included nine eyes, and the bimonthly injection group included 17 eyes. Inclusion criteria included age over 50 years, subfoveal lesions with CNV secondary to neovascular AMD or PCV cases diagnosed according to fluorescein angiography (FA) depending on the classification of previous paper [26] and indocyanine green angiography (IA). Patients who received previous AMD treatments and any retina surgery or vitrectomy history were excluded.

The Institutional Review Board of Shiga University of Medical Science Hospital approved this study, which is registered at http://www.umin.ac.jp (No. UMIN000005691). All patients provided informed written consent before participation.

Treatment and aqueous humor preparation

Anesthesia was induced using topical 4 % xylocaine before the intravitreal injections were administered. A sterile lid speculum was used in all cases. The ocular surface was prepared using a povidone–iodine solution. Undiluted aqueous humor samples were obtained from the eyes using a 29-gauge needle, followed by an IVR injection (0.5 mg/ 0.05 ml). The samples were stored at −80 °C until analysis. Patients were treated with a topical ophthalmic antibiotic four times daily starting 3 days before the day of injection and continuing for 3 days after the injection.

Measurement of VEGF concentrations

Aqueous VEGF concentrations were measured using an enzyme-linked immunosorbent assay (ELISA) (Quantikine Human VEGF Immunoassay, R&D Systems, Minneapolis, MN, USA), according to the manufacturer's instructions [16]. The lowest detectable limit of the VEGF concentration was 9.0 pg/ml.

Measurement of ranibizumab concentrations

Aqueous ranibizumab concentrations were measured by ELISA. Ninety-six-well plates were coated with recombinant human VEGF165 (R&D Systems) at a concentration of 1.0 μg/ml (100 μl/well) overnight at 4 °C. After washing three times with phosphate-buffered saline (PBS) containing 0.05 % Tween-20, the wells were blocked with 3 % bovine serum albumin (BSA)/PBS overnight at 4 °C (200 μl/well). The wells then were washed five times with PBS containing 0.05 % Tween-20 and stored dry at 4 °C for later use. Aqueous humor samples diluted in 0.1 % BSA/PBS were added to the plates overnight at 4 °C (50 μl/well). Ranibizumab was detected by horseradish peroxidase-goat anti-human IgG/F(ab')2 (Pierce Biotechnology Inc., Rockford, IL, USA) at a concentration of 1 μg/ml after a 2-hour incubation at room temperature. After five washes, color development was performed with a 100 μl 3, 3', 5, 5"-tetramethylbenzidine substrate, and the reaction was stopped by adding 1 M hydrogen chloride (100 μl). The optical density was measured at 450 nm with correction at 570 nm. The minimal quantifiable concentration of ranibizumab in the aqueous humors was 15.6 pg/ml. Because the sample volumes were small, we diluted them to 10 times and carried out the measurement. Therefore, the lowest detectable limit of the ranibizumab concentration was 156 pg/ml (0.156 ng/ml).

Examinations

The best-corrected VA (BCVA) and the central retinal subfield thickness (CRST) were measured before and monthly after the initial intravitreal injection. The BCVA was measured using a Landolt C chart and converted to the logarithm of the minimum angle of resolution (logMAR) VA and analyzed. The CRST was measured using spectral-domain optical coherence

tomography (SD-OCT) (Cirrus HD-OCT, Carl Zeiss Meditec, Dublin, CA, USA). The average retinal thickness in the central 1-mm area obtained from the macular thickness analysis was analyzed. In all eyes, FA and IA were performed before the first injection.

Statistical analysis

Statistical analysis was performed using the Sigma Stat statistical software version 3.1 (Systat Software Inc., Richmond, CA, USA). One-way repeated measures analysis of variance, Friedman repeated-measures analysis of variance by ranks, or the paired *t*-test was used to compare the differences in the aqueous VEGF concentrations, BCVA, and CRST before and after the IVR injections. $P<0.05$ was considered significant. A VEGF concentration below the lowest detectable limit was calculated as 0 pg/ml when the data were calculated.

Results

The baseline characteristics of the study patients are summarized in Table 1. No major differences were found between the two study groups except for the baseline aqueous concentration. According to the classification as published previously [26], in the monthly injection group, seven eyes of nine patients were diagnosed with neovascular AMD, including two eyes with a minimally classic lesion and five eyes with an occult lesion with no classic lesions identified by fluorescein angiography (FA); the other two eyes were diagnosed with PCV, which was identified by indocyanine green angiography. In the bimonthly injection group, 13 eyes of 17 patients were diagnosed with typical AMD (one eye with a predominantly classic lesion, four eyes with minimally classic lesions, and eight eyes had occult and no classic lesions identified by FA). The other four eyes were diagnosed with PCV.

In the monthly injection group, the aqueous VEGF concentrations ranged from 47.2 to 155.1 pg/ml (mean±standard deviation [SD], 94.7±32.0 pg/ml) at baseline, and decreased to below the lowest detectable limit in eight of nine eyes and 64.5 pg/ml in one of nine eyes at month 1 (1 month after the first injection) and decreased to below the lowest detectable limit in seven of nine eyes, 17.7 pg/ml and 58.9 pg/ml in the other two eyes respectively at month 2 (1 month after the second injection). The aqueous VEGF concentration in the monthly injection group decreased significantly ($P<0.001$, for both comparisons) at months 1 and 2 (Fig. 1).

In the bimonthly injection group, the aqueous VEGF concentrations ranged from 41.9 to 380.7 pg/ml (mean±SD, 152.4±80.1 pg/ml) at baseline and decreased to below the lowest detectable limit in two eyes at month 2 (2 months after the first injection). The aqueous VEGF concentrations ranged from 10.3 to 216.1 pg/ml (mean±SD, 69.4±60.9 pg/ml) in 15 of 17 eyes at month 2, and decreased significantly at month 2 ($P<0.001$, Fig. 2).

Table 1 Baseline characteristics of the study patient

	Monthly injection group ($n=9$)	Bimonthly injection group ($n=17$)	*P* value
Age, years	67.9±8.5	73.0±9.3	0.18
Sex, male/female	8/1	12/5	0.38
VA	0.66±0.32	0.44±0.42	0.09
CRST, μm	398.4±207.3	363.1±84.1	0.66
Aqueous VEGF concentration, pg/ml	94.7±32.0	152.4±80.1	0.02
Prior therapy for AMD	No	No	–
PCV patients	2	4	–

The ranibizumab concentrations in the monthly injection group ranged from 9.0 to 163.0 ng/ml (mean±SD, 71.2±48.6 ng/ml) at month 1 (1 month after the first injection) and from 16.3 to 222.7 ng/ml (mean±SD, 96.3±65.4 ng/ml) at month 2 (1 month after the second injection). The ranibizumab concentrations in the bimonthly injection group ranged from 0.2 to 6.9 ng/ml (mean±SD, 2.5±2.2 ng/ml) in fifteen of 17 eyes, and were below the lowest detectable limit in the other two of 17 eyes at month 2 (2 months after the first injection) (Fig. 3). When the ranibizumab and VEGF concentrations were evaluated, the aqueous VEGF concentration decreased and the aqueous ranibizumab concentration increased, with the exception of a few cases. An aqueous ranibizumab concentration of about 5 ng/ml or greater seemed to suppress the aqueous VEGF concentrations to below the lowest detectable limit (Fig. 4).

The mean logMAR BCVA values in the monthly injection group were 0.66±0.32 at baseline, 0.69±0.35 at month 1, and 0.61±0.33 at month 2 (95 % confidence interval: −0.15 to

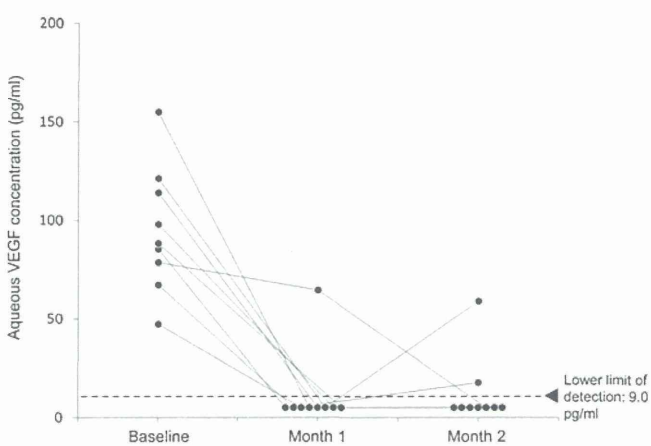

Fig. 1 The aqueous VEGF concentrations in eyes treated with monthly IVR injections. The VEGF concentrations decrease significantly ($P<0.001$ for both comparisons) after IVR injections at months 1 and 2

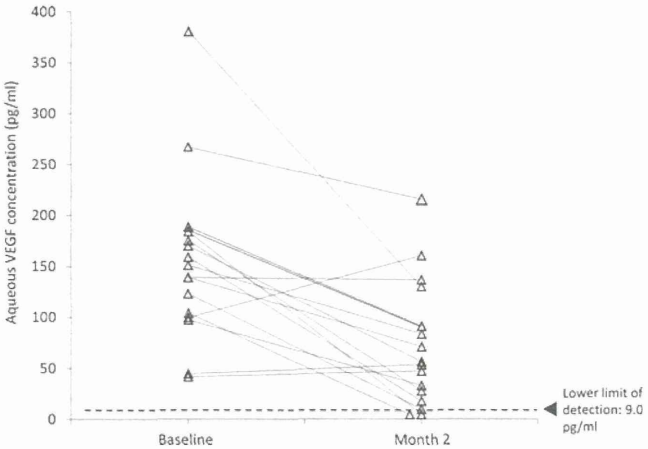

Fig. 2 The aqueous VEGF concentrations in eyes treated with bimonthly IVR injections. The VEGF concentrations decrease significantly ($P<0.001$) after IVR injections

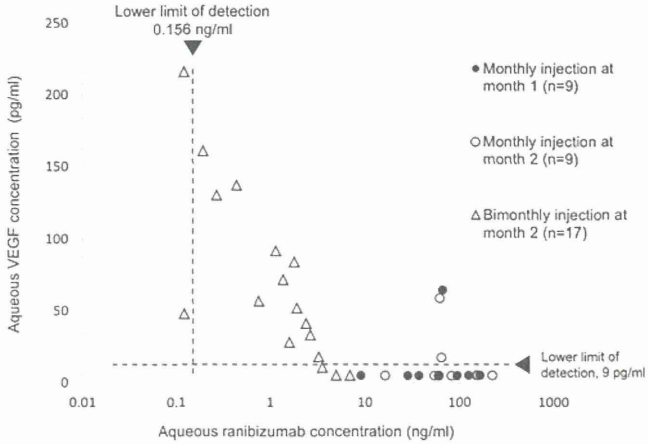

Fig. 4 Correlation between aqueous VEGF and ranibizumab concentrations in eyes treated with monthly and bimonthly injections. With a few exceptions, the aqueous VEGF level decreases and the aqueous ranibizumab concentration increases. Since the ranibizumab concentration increases to 5 ng/ml or higher, most aqueous VEGF is suppressed below the lowest detectable limit

0.10 and −0.07 to 0.18, baseline versus month 1 and baseline versus month 2 respectively). No significant differences were found in the logMAR BCVA in the monthly injection group at baseline and after treatment. The mean logMAR VA values in the bimonthly injection group were 0.44±0.42 at baseline, 0.40±0.41 at month 1, and 0.36±0.40 at month 2 (95 % confidence interval, −0.03 to 0.10 and −0.12 to 0.16; baseline versus month 1 and baseline versus month 2 respectively). The VA tended to improve, although there were no significant differences between baseline and months 1 or 2 in the two treatment groups (Fig. 5a).

The mean CRST values in the monthly injection group were 398±207 μm at baseline, 262±77 μm at month 1, and 221±60 μm at month 2 (95 % confidence interval, −33.78 to 305.78 and 29.59 to 325.96, baseline versus month 1 and baseline versus month 2 respectively). The CRST value in the monthly injection group at month 1 decreased significantly ($P<0.05$) compared with baseline. In the bimonthly injection group, the mean CRST values were 363±84 μm at baseline, 263±72 μm at month 1, and 297±103 μm at month 2 (95 % confidence interval: 70.25 to 130.93 and 17.45 to 114.31, baseline versus month 1 and baseline versus month 2 respectively). The CRST decreased significantly ($P<0.05$) at month 1 compared with baseline. The differences in the CRST values between baseline and months 1 and 2 in the bimonthly injection group were significant ($P<0.001$ for both comparisons) (Fig. 5b).

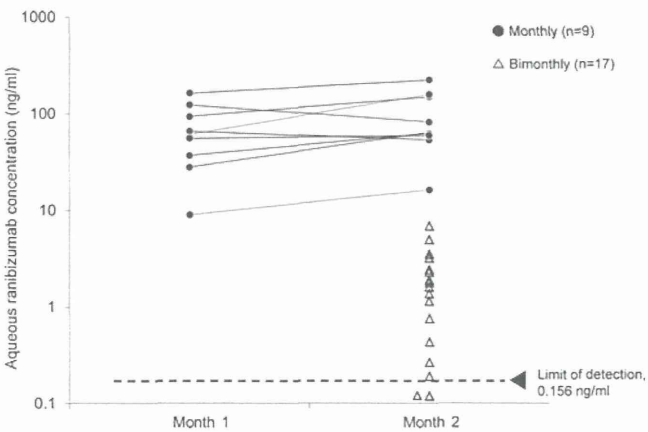

Fig. 3 The ranibizumab concentrations in eyes treated with monthly and bimonthly injections of the drug. The lowest detectable limit is 0.156 ng/ml. Ranibizumab is detectable in eight eyes treated with bimonthly injections

Discussion

To the best of our knowledge, the current study was the first to analyze the levels of aqueous VEGF and ranibizumab in eyes with AMD treated with bimonthly IVR injections. Ranibizumab was detected for at least 2 months, and aqueous VEGF concentrations decreased significantly 2 months after the first bimonthly IVR injection in most eyes. We measured the VEGF concentration in the aqueous humor rather than the vitreous humor because of the high correlation between aqueous and vitreous levels of VEGF [27–29] and ease and lower risk of obtaining aqueous humor samples compared with vitreous samples.

In the current study, the baseline VEGF level of two groups has a significant difference ($P=0.02$) which may result from the small and uneven number of patients in this study and from coincidence.

The aqueous VEGF was completely suppressed (decreased to the lower limit of detection) with monthly IVR injections, similar to previous reports [14–16]. Meanwhile, in eyes that received bimonthly IVR injections, a significant decrease in the VEGF level also was observed in 14 (82.3 %) patients at month 2, although the aqueous VEGF concentrations in only two eyes (11.8 %) were suppressed completely. The